ACADEMIC PRESS

Available online at www.sciencedirect.com
SCIENCE DIRECT®

Journal of Catalysis 215 (2003) 1–6

JOURNAL OF CATALYSIS

www.elsevier.com/locate/jcat

Features and mechanism of atomic oxygen radical anion emission from yttria-stabilized zirconia electrolyte

Masateru Nishioka,[a] Yoshifumi Torimoto,[b,*] Hodeo Kashiwagi,[a] Quanxin Li,[a] and Masayoshi Sadakata [a]

[a] *Department of Chemical System Engineering, School of Engineering, The University of Tokyo, 7-3-1 Hongo, Bunkyo-ku, Tokyo 113-8656, Japan*
[b] *Production Technology Institute of Kao Corporation, 1334 Minato, Wakayama 640, Japan*

Received 7 May 2002; revised 3 September 2002; accepted 13 September 2002

Abstract

Anion and electron emissions from Y_2O_3-stabilized ZrO_2 (YSZ) electrolyte were investigated by time of flight (TOF) spectroscopy. The atomic oxygen radical anion (O^-) is the only anion species emitted from the YSZ surface. The emission branch ratio between O^- and electrons is close to one. The Arrehenius plots for both O^- and electron emission, derived from the temperature dependences, exhibit double linear behavior. The apparent activation energies in the low-temperature region (< 620 °C) are significantly higher than those in the high-temperature region (> 620 °C). It was also found that the extraction field can enhance the O^- emission. The maximum emission current density for O^- is 3.5 nA/cm^2 in our investigated range. The observed O^- and electron emissions are attributed to the dissociation of the intermediate anions, O^{2-}, present on the YSZ anode surface. The rate-determining step for the O^- emission is believed to be the desorption process in the low-temperature region, and the electron desorption or the electrochemical reaction in the high-temperature region.

1. Introduction

In recent years, negative ion implantation has been utilized as a new means of surface modification because the features of negative ions have been revealed to be very different from those of positive ions [1–6]. Due to negative charge polarity and the low energy of electron affinity, implantation and deposition using negative ion beams is more favorable to neutralization in comparison with that using positive ion beams. In the case of negative ion implantation in large integrated chips, a technology for fabricating gate insulators without any damage has been achieved due to lack of surface charge-up during the operation [1–3]. When negative ions are used for ion beam disposition, ceramic films with high density can be prepared [4]. On the other hand, the atomic oxygen radical anion (O^-) is one of the key chemical species in combustion and the oxidation of biochemical materials due to its high oxidativity [7,8]. In spite of various potential applications of negative ions in materials science and chemistry, there are only a few methods for producing negative ions, such as discharge, electron detachment, and ion bombardment. These methods are far inferior from the viewpoint of energy efficiency and selectivity for producing a specific negative ion.

A new approach to extracting atomic oxygen radical anions has been reported by our research group [9,10]. It was found that O^- emission to the gas phase can be achieved by simply applying an electronic field between the Y_2O_3-stabilized ZrO_2 (YSZ) anode and the space electrode and supplying oxygen and electrons opposite to the emission surface. We also found that highly energy-efficient production of O^- can be further improved using a microstructure design, where the input power is decreased without changing the O^- emission intensity [23]. Although we have studied the O^- emission from the YSZ electrolyte, many features and the emission mechanism remain to be revealed. In the present work, we present quantitative studies of the O^- and electron emissions using our new developed time of flight system. The emission behavior, including the emission branch ratio between O^- and electrons, the absolute emission current density, the temperature, and the extraction field effects have been studied. Based on various

* Corresponding author.
E-mail address: torimoto.yoshifumi@kao.co.jp (Y. Torimoto).

0021-9517/03/$ – see front matter
doi:10.1016/S0021-9517(02)00041-6

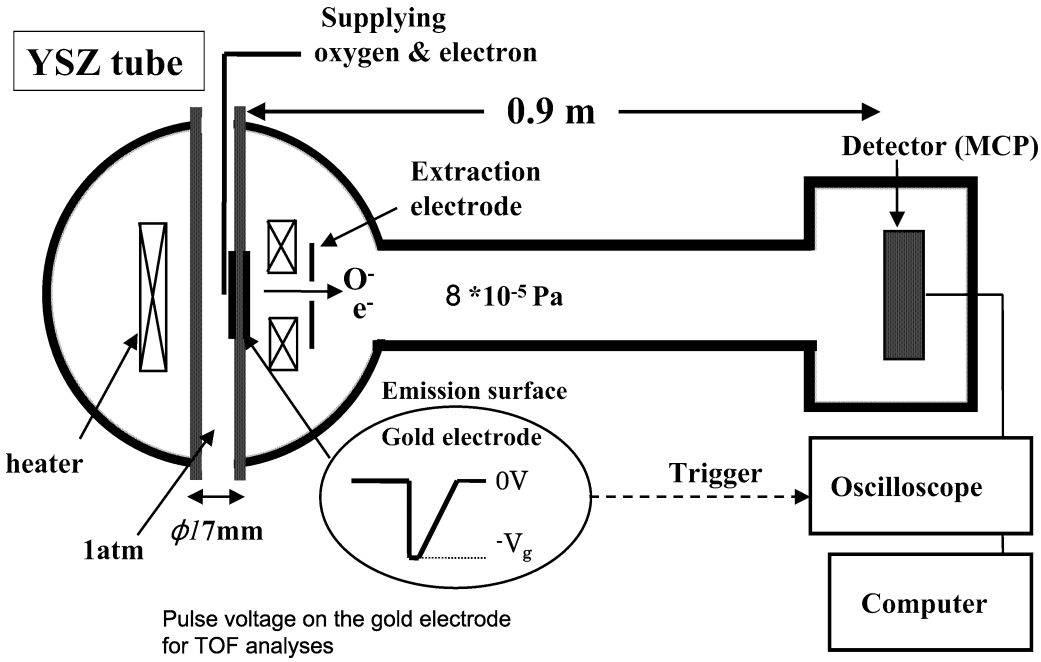

Fig. 1. Schematic diagram of the experimental apparatus, which mainly consists of two sections: a sample chamber and an ion-detection chamber mounted on a time of flight (TOF) mass spectrometer for measuring the emitted anions and electrons from the treated YSZ electrolyte surface.

investigations, the mechanism for the O^- and electron emission from the YSZ anode will be addressed.

2. Experimental

In this study, a commercially used cylindrical YSZ specimen (Nikkato Corp.) with outer diameter 17 mm, thickness 3 mm, and length 600 mm was used. A thin and uniform golden film with a length of 10 mm, was made on the outside surface of the YSZ tube center, which was used as an anionic emission surface. The inside wall of the tubular YSZ was also coated with Au paste. Then the specimen was dried at 500 °C for 1 h and calcined at 800 °C. In order to eliminate impurities on the emission surface, the specimen was treated at 800 °C for 8 h under flowing dried air.

A schematic diagram of the experimental setup is shown in Fig. 1. The experimental apparatus mainly consists of two sections: a sample chamber and an ion-detection chamber with a time of flight (TOF) mass spectrometer, which are pumped by two turbo molecular pumps (typical vacuum $\sim 1.3\times10^{-3}$ Pa). The treated YSZ specimen was installed in the sample chamber with a diameter of 0.4 m The emission surface, located in the center of the sample chamber, was opposite to the ion detector and heated radiatively by an Fe–Cr alloy filament. The heater was quartz-sealed in order to avoid any electron emission from it. The surface temperature was measured by a Ni/Ni/Cr thermocouple. In order to continuously inject the O^{2-} into the YSZ electrolyte, we supplied the electron and oxygen on the inside surface of the YSZ tube, where the O^{2-} was generated by the electrocatalytic reaction of O_2 to O^{2-}, i.e., $\frac{1}{2}O_2(g)+2e^-\rightarrow O^{2-}$ [12–14]. The formed O^{2-}, then, transfers through the YSZ solid electrolyte into the emission surface (in the vacuum) by field-enhanced thermal diffusion. The anions and electrons emitted from the surface were extracted by an extraction electrode which is mounted in the opposite of the emission surface with a changeable distance from 1 to 5 cm. The extraction field strength was determined by the applied potential on the emission surface and the distance between the emission surface and the extraction electrode. The anionic collection electrode was collected to a picoammeter for total emission current measurement. In the center of the collection plate, there was a 0.2-mm pinhole, which allows simultaneous analysis by a TOF spectrometer.

The emitted anions and electrons were analyzed by the TOF spectrometer, which was pumped by another turbomolecular pump system. The TOF spectrometer, which has flight length 0.9 m, was mounted on two multichannel plates (MCP) and operated in the pulsed negative ion detection mode. The output signal of the MCP was amplified by an amplifier (100 times), recorded by a digital oscilloscope, and finally acquired by a computer-controlled counter system. The collection efficiency was calibrated by changing the length of TOF and the size of the sampling pinhole (normally, we adopted a pinhole of 0.2 mm for the TOF measurements). In order to check the possible contribution to the O^- signal arising from surface or gas phase reactions in the sample chamber, we have investigated the O_2 pressure dependences of the anion emission. The results show that the intensity of O^- is nearly constant in the O_2 pressure range between 10^{-2} and 10^{-3} Pa. More important, no products were observed in the TOF spectra. Thus it is believed

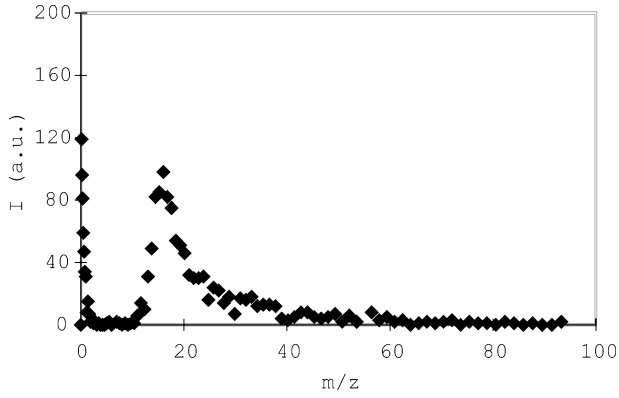

Fig. 2. Typical TOF mass spectrum of negative ions emitted from the YSZ surface at 580 °C and 500 V/cm.

that the reactions of the gas phase and surface can be negligible under our experimental conditions.

3. Results and discussion

Before the YSZ electrolyte was heated, the sample chamber was pumped to $\sim 10^{-3}$ Pa so that the gas phase reaction was negligible. The leak current has been carefully checked; it was also negligible under our experimental conditions. No ions were observed at room temperature. For surface temperatures over 450 °C, anion and electron emissions can be detected both by the picoampere meter and the TOF spectrometer.

The anionic species emitted from the treated YSZ electrolyte surface were investigated by time of flight mass spectrometer. As shown in Fig. 2, only two peaks have been observed in all TOF mass spectra. One peak, located at the mass number of 16, corresponds to the O^- anions emitted from the surface. Another peak, corresponding to flight times close to zero, is the emitted electron.

At surface temperatures lower than 400 °C, no anionic emission was observed within our experimental sensitivity. Both O^- and electron emission gradually increase with increasing surface temperatures over 450 °C. Fig. 3 and 4 clearly show that both the O^- and electrons emitted from the YSZ anode are strongly dependent on the surface

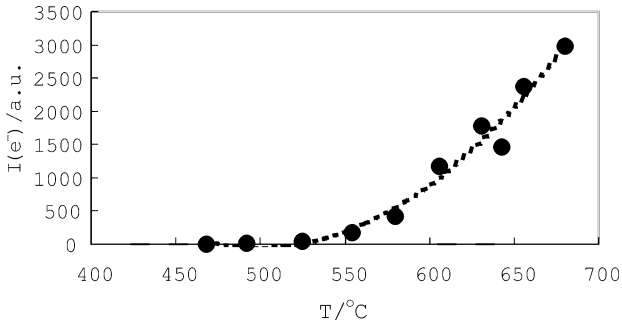

Fig. 3. Temperature dependence of the O^- emission at a given extraction field of 500 V/cm.

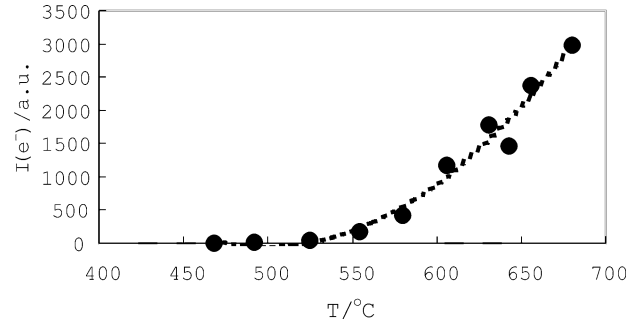

Fig. 4. Temperature dependence of the electron emission at a given extraction field of 500 V/cm.

temperature. In order to derive the apparent activation energy for the O^- emission, the temperature dependences are also plotted by Arrehenius type, i.e., $\ln I \sim 1/T$. As shown in Fig. 5, our results indicate that the Arrehenius plot cannot be described by a straight line. Alternatively, it is more suitably described by double lines in the high-temperature region (> 620 °C) and the low-temperature region (< 620 °C), respectively. Therefore, we obtained two apparent activation energies, expressed by E_{LT} and E_{HT}, for the low-temperature region (450–620 °C) and the high temperature region (620–750 °C). The data are summarized in Table 1. The apparent activation energies in the low-temperature region are obviously higher than those in the high-temperature region. This phenomenon may indicate that the anion emission is a series process (i.e., multistep process), as will be discussed in detail in next section. Similar temperature behavior is also observed for electron emission from the YSZ anode surface (see Fig. 6). Furthermore, it was found that the apparent activation energies can be reduced by the extraction field (see Table 1).

The emission intensities of the O^- and electrons are also sensitive to the applied extraction field. Typical field dependences of the O^- and electron are presented in Figs. 7 and 8 at a given temperature of 656 °C. When the field is less than 150 V/cm, the emission is very weak and negligible. When the extraction field is increased, the emission intensity progressively increases with the field over a certain threshold. It should be pointed out that the field behavior could not be attribute to the detection efficiency of the TOF spectrome-

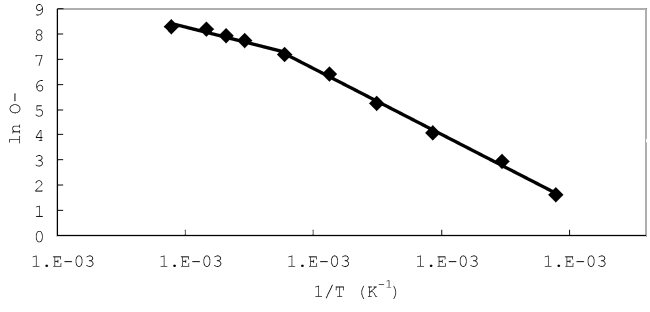

Fig. 5. Arrhenius plot for emitted O^- at 500 V/cm. It exhibits double-line behavior and has larger apparent activation energy in the low-temperature region (450–620 °C).

Table 1
Activation energies of O^- and e^- measured at different extraction fields

V/cm	$E_{LT}(O^-)$	$E_{HT}(O^-)$	$E_{LT}(e^-)$	$E_{HT}(e^-)$
300	263.9	89.1	214.3	158.9
400	208.9	77.1	220.5	128.4
500	217.1	85.5	225.4	91.1
600	212.0	63.2	202.3	72.8
700	201.3	79.5	198.2	79.0
800	203.9	58.7	184.1	62.7

LT and HT stand for the apparent activation energies measured in the low-temperature region (450–620 °C) and the high-temperature region (620–750 °C), respectively. The unit of the activation energy is kJ/mol.

ter, because the space emission current, detected even at a close distance of 1 cm from the emission surface, exhibits similar field effects (see Fig. 9). As explained below, the observed O^- and electron emission originate from the dissociation of the intermediate anion O^{2-}, which occurs on the YSZ anode emission surface. The O^{2-} coverage on the emission surface is increased by the applied external field because the migration of the O^{2-} from the bulk into the emission surface should be enhanced. On the other hand, the applied field may reduce the surface barrier height because, to leave the surface, anions must possess translation energy in excess of the potential which binds them to the surface. Our results indeed confirm that the apparent activation energy can be decreased by the applied field.

The absolute emission current density has been measured simultaneously by a picoampere meter. The results are shown in Figs. 9a and b. As mentioned above, the emission current density shows temperature and field effects similar to those measured by TOF mass spectroscopy. The maximum emission current density is 7 nA/cm^2 at 750 °C and 1500 V/cm in our investigated region. On the other hand, the emission branch ratio of O^-, r, defined as the ratio of O^- to total anions and electrons emitted, is about 0.5, and is independent of the temperature in our investigated range (Fig. 10).

The various investigations mentioned lead us to consider the emission mechanism of O^- and electrons observed. It is well known that Y_2O_3-stabilized ZrO_2 (YSZ) electrolytes possess high ionic conductivity for anion O^{2-} [11–20]. Although the anion O^{2-} can exist in the bulk of the YSZ electrolyte, no evidence of O^{2-} was found in the gas phase according to our investigation. This implies that the transient O^{2-} is very unstable on the electrode surface. As for functions of the Au anode on YSZ relating to the dissociative adsorption of oxygen, no effects were observed in the paper [9] reported by the authors. Therefore, the following mechanism is considered to explain the observed electron and O^- emission. The anions of O^{2-} form initially by the electrocatalytic reaction $\frac{1}{2}O_2(g) + 2e^- \rightarrow O^{2-}(s)$, by the supplied oxygen and electrons on the Au-coated YSZ electrolyte (the inside surface of the YSZ tube) [12–14]. After the O^{2-} anions migrates into the emission surface by electronic-field-enhanced thermal diffusion, rapid dissociation of O^{2-} into O^- and e^- will occur on the emission surface. Finally, the dissociation products, O^- anions and electrons, will eject into vacuum though the three phase boundary (Au–YSZ–vacuum boundary) or the Au surface. This series emission processes can be expressed by

$$\begin{aligned} O_2(g) + e^- &\rightarrow O^{2-} \text{ (inside surface of YSZ electrolyte)} \\ &\rightarrow O^{2-} \text{ (bulk of YSZ)} \\ &\rightarrow O^{2-} \text{ (emission surface)} \\ &\rightarrow O^- \text{ (emission surface)} \\ &\quad + e^- \text{ (emission surface)} \\ &\rightarrow O^- \text{ (space)}\uparrow + e^- \text{(space)}\uparrow . \end{aligned}$$

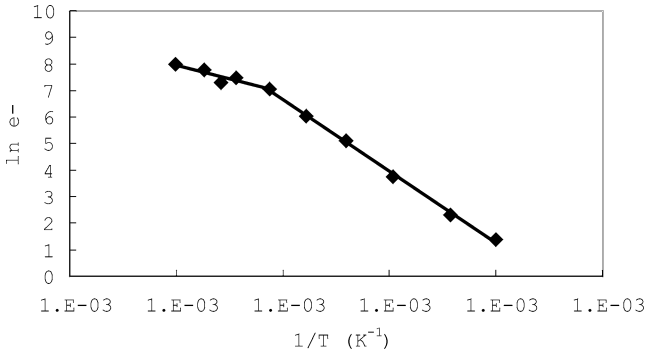

Fig. 6. Arrhenius plot for emitted electrons at 500 V/cm. The double line behavior is also shown.

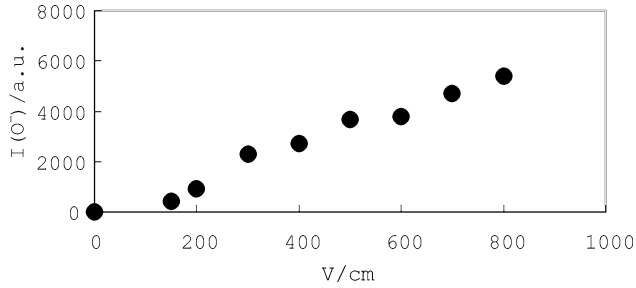

Fig. 7. Extraction field dependence of O^- at a given temperature of 656 °C.

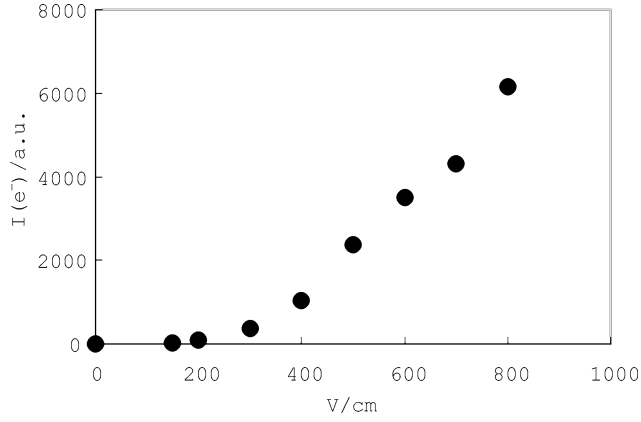

Fig. 8. Extraction field dependence of the emitted electrons at a given temperature of 656 °C.

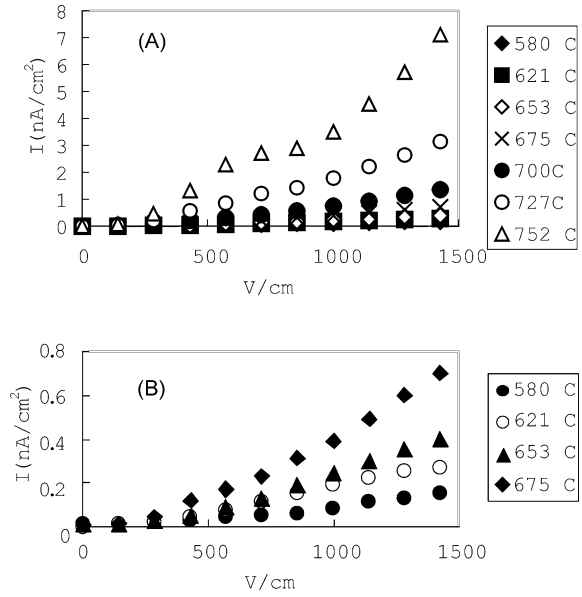

Fig. 9. The absolute emission current density versus the extraction field at a series of surface temperatures.

The above mechanism is also supported by the fact that the emissions intensity of O^- is close to that of electrons from the YSZ surface, since both O^- and electron emission originate from the same process of O^{2-} anions dissociation. We believe that only few electrons emit from the Au electrolyte surface due to the large work function of emission (5.1 eV, Ref. [24]). Hence, most of the electrons must be emitted from the three-phase boundary.

Our results show that the apparent activation energies for the O^- emission in the low-temperature region (< 620 °C) are obviously larger than those in the high-temperature region. This may imply that the rate-determining steps for the O^- emission are different at high and low temperatures. Unfortunately, the desorption activation energy of O^- from the Au surface is unknown so far. We note that the apparent activation energy for O^- emission in the low-temperature region is located in the range 204–251 kJ/mol. The values are close to the binding energy of oxygen atom on the Au surface (227–234 kJ/mol) [21,22]. Thus it seems that

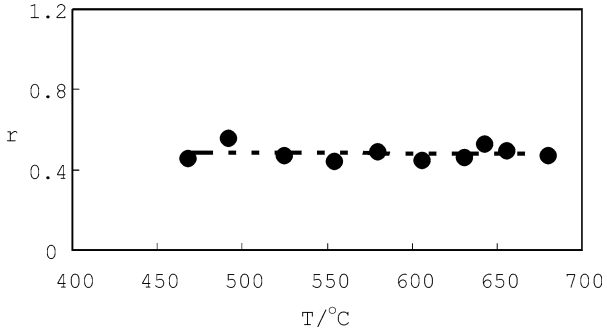

Fig. 10. The ratio of O^- to total anions and electrons emitted from the YSZ surface. The ratio is close to 0.5 and nearly independent of the surface temperature.

the O^- emission is controlled by the O^- desorption from the Au surface in the low-temperature region and by the electron desorption or the electrochemical reactions in the high-temperature region. Furthermore, three are two candidates for the desorption sites of O^-, i.e., (1) the three-phase boundary (TPB) and (2) the surface of the Au electrode. When case (1) is considered, the O^- emission process is likely to be a one-step process (i.e., O^{2-} (TPB) $\rightarrow$ O^- (TPB)$\uparrow + e^-$(TPB)$\uparrow$). This is in contradiction to the experimental result, which shows that two-step series processes exist in the O^- emission. Thus, O^- may first migrate from the three-phase boundary to the Au surface and then desorb from the Au surface, which can be expressed by the following two-step series processes:

$$O^{2-} \rightarrow O^-(\text{TPB}) \rightarrow O^-(\text{Au-electrode})\uparrow .$$

4. Conclusion

This work has contributed to the study of the emission features and mechanisms that govern O^- emergence into vacuum from the treated Y_2O_3 stabilized ZrO_2 (YSZ) electrolyte surface. We observed that the O^- emission is strongly dependent both on the surface temperature and the extraction field. The emission ratio between O^- and electrons is near one. The O^- emission is considered to originate from the dissociation of the transient anions of O^{2-}, which form initially by an electrocatalytic reaction between the supplied oxygen and electrons. After the O^{2-} anions transfer onto the emission surface of the YSZ electrolyte by external-field-enhanced thermal diffusion, rapid dissociation will take place, and finally desorb into vacuum as free O^- (in the gas phase). In particular, the Arrehenius plots show double line behavior, which exhibits higher apparent activation energies at temperatures lower than about 620 °C. This behavior indicates that the rate-determining steps are different in the high- and low-temperature regions. The O^- emission is controlled by the O^- desorption process from the Au surface in the low-temperature region, and by electron desorption or the electrochemical reaction in the high-temperature region.

Acknowledgments

This work was supported by the core research for evolutionary science and technology in JST (Japan Science and Technology). We are grateful to Professor Hosono and Dr. Yamanishi for their motivating discussions in this work.

References

[1] J. Ishikawa, H. Tsuji, Y. Toyota, Y. Gotoh, K. Matsuda, M. Tanjyo, S. Sakai, Nucl. Instrum. Methods Phys. Res. B 96 (1995) 7.
[2] J. Ishikawa, Surf. Coat. Technol. 65 (1994) 64.

[3] J. Ishikawa, Rev. Sci. Instrum. 65 (1994) 1290.
[4] J. Ishikawa, Rev. Sci. Instrum. 17 (2000) 2.
[5] M. Tanaka, K. Amemiya, Rev. Sci. Instrum. 71 (2000) 1125.
[6] G.D. Alton, Y. Mori, A. Takagi, A. Ueno, S. Fukumoto, Nucl. Instrum. Methods A 270 (1988) 194.
[7] J. Lee, J.J. Grabowski, Chem. Rev. 92 (1992) 1611.
[8] K. Aika, J.H. Lunsford, J. Phys. Chem. 81 (1977) 14, 1393.
[9] Y. Torimoto, A. Harano, T. Suda, M. Sadakata, Jpn. J. Appl. Phys. 36 (1997) L238.
[10] Y. Torimoto, K. Shimada, T. Nishioka, M. Sadakata, J. Chem. Eng. Japan 33 (2000) 557.
[11] C.G. Vayenas, S. Bebelis, S. Ladas, Nature (London) 343 (1990) 625.
[12] C.G. Vayenas, D. Tsiplakides, Surf. Sci. 467 (2000) 23.
[13] C.G. Vayenas, A. Ioannides, S. Bebelis, J. Catal. 129 (1991) 67.
[14] C.G. Vayenas, S. Bebelis, I.V. Yentekakis, H.G. Lintz, Catal. Today 11 (1992) 303.
[15] D.Y. Wang, A.S. Nowick, J. Electrochem. Soc. 128 (1981) 55.
[16] W. Zipprich, H.D. Wiemhofer, U. Vohrer, W. Gopel, Ber. Bunsenges. Phys. Chem. 99 (1995) 1406.
[17] S. Ladas, S. Bebelis, C.G. Vayenas, Surf. Sci. 251/252 (1991) 1062.
[18] J. Nicole, D. Tsiplakides, S. Wodiunig, C. Comninellis, J. Electrochem. Soc. 144 (1997) 1312.
[19] J. Poppe, J. Shaak, J. Janek, R. Imbihl, Ber. Bunsenges. Phys. Chem. 102 (1998) 1019.
[20] J. Poppe, S. Volkening, A. Schaak, E. Schutz, J. Janek, R. Imbihl, Phys. Chem. Chem. Phys. 1 (1999) 5241.
[21] H. Hakkinen, U. Landman, J. Am. Chem. Soc. 123 (2001) 9704.
[22] N. Saliba, D.H. Parker, B.E. Koel, Surf. Sci. 410 (1998) 270.
[23] Unpublished data.
[24] C. Jackschath, I. Rabin, W. Schulze, Ber. Bunsenges. Phys. Chem. 96 (1992) 1200.